Research Article

Journal of Environmental Nanotechnology

Unleashing the Flexural Behavior of Ceramic Hybrid Rubber Reinforced Composites for Sustainable Industry

P. Subashree[1*], S. Vivek[2] and N. Muthukumaran[3]

[1]Department of Civil Engineering, Sri Krishna College of Technology, Coimbatore, TN, India
[2]Department of Civil Engineering, GMR Institute of Technology, Rajam, AP, India
[3]Department of Civil Engineering, V. S. B. College of Engineering Technical Campus, Coimbatore, TN, India

Received: 01.02.2024 Accepted: 27.03.2024 Published: 30.03.2024

*subashree.p@skct.edu.in

ABSTRACT

An innovative methodology is employed to explore the potential of repurposing floor ceramics and used tire rubber for fine aggregate. In contrast to one-way ordinary concrete slabs, the behavior of Ceramic Hybrid Rubber Reinforced Composite Slabs (CHRRCS) under pure bending has been thoroughly examined. There is no discernible negative effect of the quantity of ceramic floor tiles on the characteristics of concrete. In this study, M30 concrete with a water-to-cement ratio of 0.38 is employed. The distribution reinforcement was made up of bars with an 8 mm diameter, while the main reinforcement was made up of 10 mm diameter Fe 415 grade steel bars. The CHRRCS with 2% rubber fibers, 10% replacement ceramic, and 10% pre-treated crumb rubber exhibit more significant deflection only under extreme stress conditions. Apart from the experimental study, ABAQUS was used to perform a finite element model in three-dimensional simulation and analyze the load-displacement behavior. The comparison of ABAQUS simulation and experimental data yields a fair range. The flexural performance of CHRRCS is enhanced in pure bending.

Keywords: Ceramic; Hybrid rubber reinforced composite slabs; Flexural strength; One-way slab; Crumb rubber.

1. INTRODUCTION

Repurposing ceramic tiles and used rubber tires as aggregates offers sustainable solutions for construction. These materials, when processed and combined, provide durable and environmentally friendly alternatives for various applications. By diverting waste from landfills and reducing the demand for virgin resources, such initiatives promote eco-conscious building practices (Zamora *et al*. 2021). Concrete with a 30% replacement of waste ceramic particles has high axial strength (Awoyera *et al*. 2016). Kim *et al*. (2015) concentrated on pozzolanic filler in concrete made of old ceramic tiles. Vejmelková *et al*. (2012) substituted concrete samples with ceramic floor tiles to varied degrees (10%, 20%, 30%, and 40%). When water absorption and compressive strength were tested with a 20% increase in ceramic floor tiles, no discernible negative effects on concrete's compressive strength were seen (Rashid *et al*. 2017).

One of the most persistent environmental problems (EPA, 1991) in the world is rubber waste from tires. Not only are old tires disposed of, but also additional garbage from car manufacturers (Camille *et al.* 2013). Many governments have banned the dumping of waste tire rubber in landfills due to the ongoing shortage of accessible disposal sites. In order to stop this depletion and develop suitable waste tire disposal methods, much research has been conducted. The energy-absorbing, flexible, lightweight, heat- and sound-absorbing qualities of recycled tire materials make them highly desirable in the construction sector (Ganesan *et al*. 2012). The usage of discarded tires in civil engineering is now relatively limited since there are few products that employ recycled tires that are used in large quantities (El-Gammal *et al.* 2010). Sara (2010) conducted engineering-related tests to identify the ideal types and amounts of aggregate for different concrete compositions. The results show that one practical way to reduce weight in some technological goods is to add rubber aggregates made from used tires to concrete (Eldin and Senouci, 1993). Despite a number of drawbacks, such as a notable decrease in compressive strengths and a rise in air content and water consumption, the trials demonstrate that rubber provides a mix with unique properties that may be advantageous in the field of construction.

2. MATERIALS & METHODS

2.1 Bending Test on HRRCS Slabs

2.1.1 Details of Slabs

As part of the experimental investigation, 18 supported rectangular slabs with dimensions of 1000 mm × 450 mm × 60 mm were examined for one-way slabs (OWS). Ceramic Hybrid Rubber Reinforced Composite Slabs (CHRRCS) and Ordinary Reinforced Concrete Slabs (ORCS) were the two primary categories of slabs.

Slab sets ORCS1 and ORCS2 were cast as conventional slab specimens, while slab hardens CHRRCS1 to CHRRCS5 were deemed as one-way slabs with designing steel reinforcement. The CHRRCS is made by pouring ordinary concrete on the bottom half of the slab and covering it with rubberized concrete according to the reinforcing design. M30 concrete has a water-to-cement ratio of 0.38, according to IS 10262:2009, with a mix percentage of 1:1.15:2.12. Figure 1 depicts the dimensions of the slab specimen. Ceramic of 10% replacement for fine aggregate is kept constant in all the mixes (Aziz and Salwa, 2011). In the current study to improve the fresh concrete characteristics and flexural behaviour, rubber fibres of varied percentages (0.5%-2.0%) for a total concrete weight were filled into the top half layer of the CHRRCS slab. Furthermore, fine aggregate was substituted for 10% of the crumb rubber (Aziz *et al.* 2010). The slenderness ratio was investigated as one of the test characteristics as CHRRCS incorporates steel reinforcement. To determine the material qualities of concrete, specimens were cast beside each set of slabs (IS 516:1959). The size of a slab is used to classify it. A one-way slab is defined as one that has a long span to short span ratio greater than two. The main reinforcement consisted of 10 mm diameter of Fe 415 grade steel bars, with distribution reinforcement consisting of 8 mm diameter bars (IS 456:2000). A clear cover of 15 mm was used to strengthen the slabs in both directions.

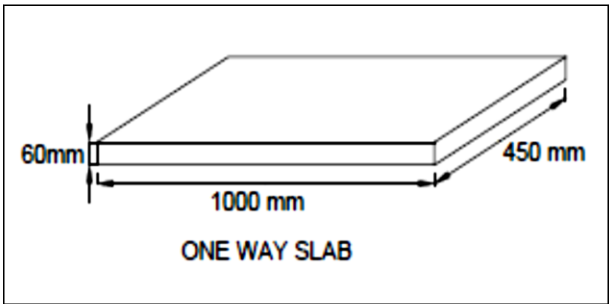

Fig. 1: Dimensions of the slab specimen

2.1.2 Test Procedure

The slabs were put through their paces in a 50-ton loading frame with a two-point load setup. The 15-ton hydraulic jack was securely connected and locked. A single Linear Variable Differential Transformer (LVDT) put in the centre of the slab was used to measure the deflection. A hydraulic jack was used to apply the weight axially. Based on the specimen's anticipated ultimate load bearing capacity, the load was increased by 2 kN. The initial readings were taken when the LVDT was installed in the slab's center and were based on loading position. The values were calculated using indices for each load, increment deflection, and strain. Each load increase was measured using LVDTs, which measure the axial and lateral displacements. The LVDT indication shows displacement in millimeters. The loading setup is shown in Fig.2 and Fig.3. The shear span is a_v, and the slab length is L.

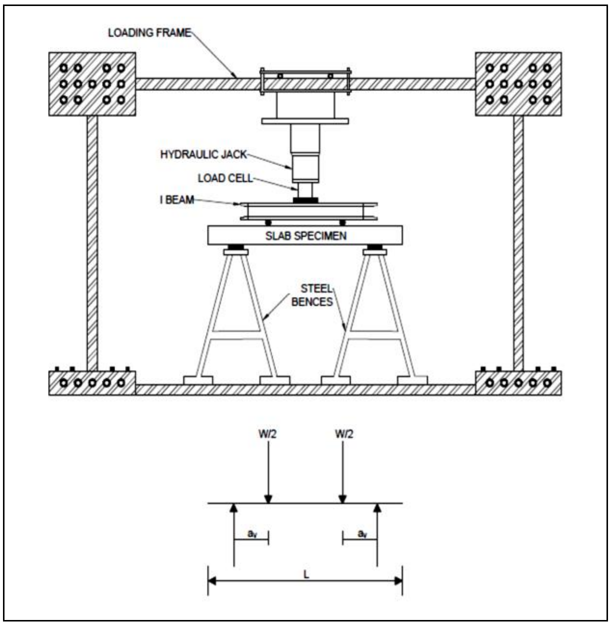

Fig. 2: Loading arrangement

Fig. 3: Experimental setup of slab

3 RESULTS & DISCUSSION

3.1 Structural Behavior of HRRC Slabs

The two types of reinforced concrete used in the construction were the ORCS and CHRRCS. The load, fracture formation and progression, compression concrete crushing, and tension steel yielding of composite slabs were compared (Ali and Ayhan, 2012). Table 1 shows the load and deflection at crucial places, as well as the failure mode. The specimens' vertical deflections at the span's center are shown using the applied load P. The applied load at both places is represented by P. Figure 4 shows the load-deflection curves for HRRC slabs. All one-way slabs deflected linearly as a result of the applied load P. There was a lot of deformation on the slab.

Table 1. Experimental results of slabs

S. No.	Slab Series	Slab Reference ID	Slab Type	Grade of concrete	Slab Dimensions (mm)	Percentage of replacement as FA	Percentage of replacement as RF	First Cracking Load (kN)	Ultimate Load (kN)	Deflection (mm)
1	ORCS1	ORCS11	OWS	M30	1000 × 450 × 60	-	-	2.64	19.3	9.29
		ORCS12				-	-	2.36	18.7	8.95
		ORCS13				-	-	2.5	19	9.12
2	CHRRCS1	CHRRCS11				10	0	2.85	21	9.3
		CHRRCS12				10	0	3.0	20	9.25
		CHRRCS13				10	0	3.15	19	9.2
3	CHRRCS2	CHRRCS21				10	0.5	3.2	22	10.52
		CHRRCS22				10	0.5	3.21	20	10.36
		CHRRCS23				10	0.5	3.19	24	10.68
4	CHRRCS3	CHRRCS31				10	1.0	3.46	20	10.35
		CHRRCS32				10	1.0	3.5	21	10.20
		CHRRCS33				10	1.0	3.54	22	10.05
5	CHRRCS4	CHRRCS41				10	1.5	4.1	23	11.02
		CHRRCS42				10	1.5	4.15	24	10.85
		CHRRCS43				10	1.5	4.05	22	11.19
6	CHRRCS5	CHRRCS51				10	2.0	5.1	25	11.42
		CHRRCS52				10	2.0	5.15	24.5	11.3
		CHRRCS53				10	2.0	5.05	25.5	11.54

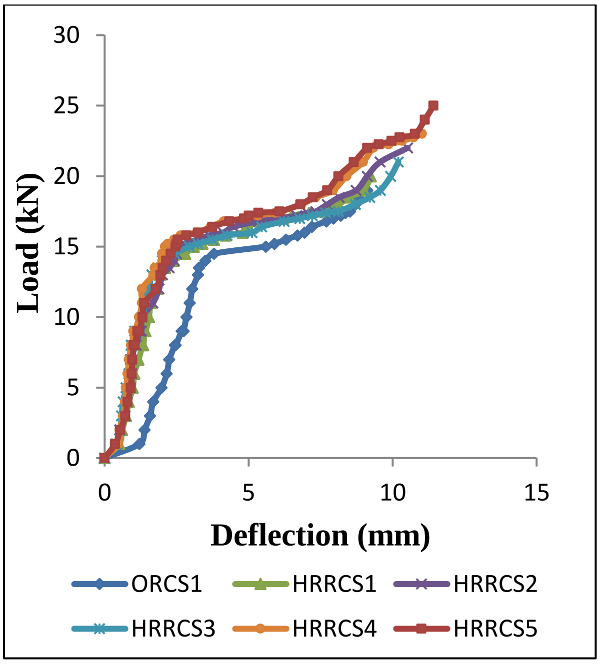

Fig. 4: Load-Deflection curves for C-HRRCS

3.2 Patterns of Cracking and Failure

Figure 5 depicts the failure modes of all slabs tested in CHRRCS mixes. All of the specimens displayed typical flexural failure due to the fact that they were designed and manufactured as CHRRCS. While conducting the test, each slab specimen collapsed. With increase in load, vertical cracks were observed from the top of the specimens. Under 2.5 kN of load and 1.5 mm of deflection, a first crack formed at the right support in the slab specimen. At 9 kN of stress and a 6 mm deflection, a crack developed in the mid-span of the slab's bottom. When 15 kN of load was acting with a 7.8 mm deflection, the third crack formed directly under roller. The final failure occurred at 19 kN of load with a 9.12 mm deflection as the width of the second and third cracks increased. When compared to the control slab ORCS1, the ultimate load of CHRRCS5 had a 31.57 % higher ultimate strength. In all slab specimens, the pattern of crack growth began around the panel's center. As the weight increased, new fractures appeared, and existing cracks continued to propagate to the corners. Because the corners were free to move, some of the fissures branched around them.

Fig. 5: Failure mode of CHRRCS

3.3 Numerical Investigation of CHRRC Slabs through Modelling and Meshing

The software ABAQUS was used to create unique sketches of concrete and steel parts that may be extruded in all directions. The slab and reinforcements are made up of different pieces. The slab is a three dimensional deformable solid, and the steel reinforcements are 3D deformable wire models of the same sort. In the assembly module, utilized for analysis, separate instances were produced. Figure 6 depicts the CHRRC slab's model based on finite elements. The bottom slab study mimics a normal concrete slab, while the top layer depicts a rubberized concrete slab. Six slabs were modelled for flexural bending. Conventional slabs were also modelled and compared to those of other slabs. When developing steel reinforcement for one-way slabs, the size and cover offered to the slabs were kept consistent at 1000 mm × 450 mm × 60 mm. The compressive and tension stiffening behaviours of grade M30 concrete are quantitatively represented. The damage parameters of the system, including those outlined in the 'Concrete Damage Plasticity' model (IS 516:1959), consist of tension damage parameters with a recovery rate of 0.01 and compression damage parameters with a recovery rate of 0.99. The modulus of elasticity, calculated as 5700 fck, and the Poisson's ratio, taken as 0.2, were used to determine the elastic properties of concrete. The steel reinforcements were modelled as elastic-plastic, with an elastic modulus of 2×10^5 GPa and a Poisson's ratio of 0.3 in the elastic range and yield stress and plastic strain in the plastic range. The Young's modulus and flexural strength of all crumb rubber aggregate concrete mixtures were calculated using experimental data. The CHRRC slabs with experimentally established dimensions and mechanical properties were modelled in the finite element analysis (FEA) (Joe and Chandler, 1992). Multiple activities were done in order for the model to operate effectively in ABAQUS while creating the FEM. A graphical user interface (GUI) was used to generate models.

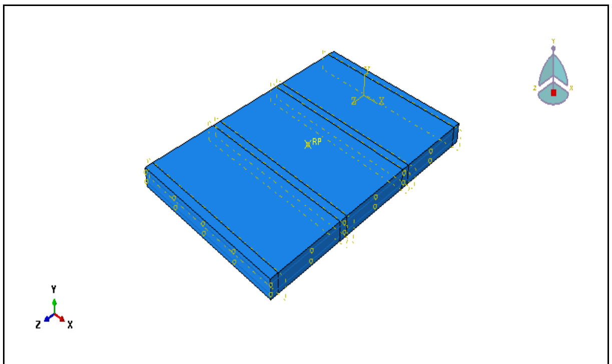

Fig. 6: 3-D Modelling of the CHRRC slab

In order for the slab to function as an CHRRC slab, the embedded region constraint creates a relationship between concrete and steel reinforcement. The full plain concrete host region was wrapped in the reinforcement. The embedded formulation allows to choose a concrete mesh that is not dependent on it. The stiffness of the reinforcing elements and the stiffness of the concrete elements were tested separately using this method. The elements were included in the concrete mesh in order for its displacements to match those of the surrounding concrete elements. The concrete elements and their intersection sites with each reinforcement segment were identified and used to calculate the nodal locations of the reinforcement elements.

C3D8R, an eight-node linear brick element with constrained integration and hourglass control, was used to produce the undamaged concrete slab. The CHRRC slabs were given material attributes such as steel, rubber, and concrete. The input file was constructed by assembling and assigning material properties, as well as establishing a meshing component for concrete, rebars, and stirrups, and a global seed to assign the mesh controls, with an approximate size for the global seed.

Connecting nodes define the elements that make up a mesh section. Figure 7 illustrates the meshing of CHRRC slab parts.

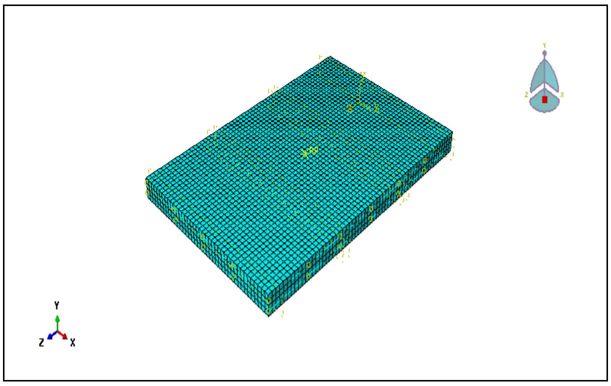

Fig. 7: Meshing of elements of the CHRRC slab

3.4 BOUNDARY CONDITIONS AND LOADING

The slab's x and y movement is limited due to the hinged supports at both ends (Al-Tayeb *et al*. 2012). Loads were applied in displacement control mode. Two-point flexural loading was employed on the ceramics hybrid rubberized composite slab. The load vs. displacement behaviour of CHRRC slabs was modelled using the ABAQUS software. Replacement of fine aggregate with crumb rubber produced one-way slab models for static bending stress analysis (Kamil *et al.* 2005). Figure 8 illustrates the CHRRC slab, as well as its loading and boundary conditions.

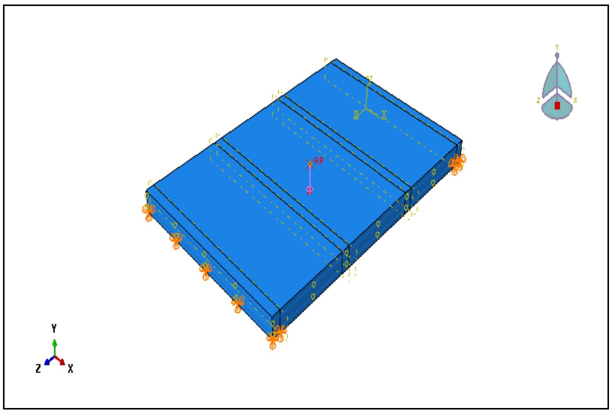

Fig. 8: Loading and boundary conditions of the CHRRC slab

3.5 COMPARISONS

Both field and historical output requests should be considered while conducting the job analysis. A data check job manager was created and submitted in order to visualise the outcomes of the entire analysis in order to solve any FEA problem. Experimental data were used to validate the proposed model. In the computational model, the CHRRC10 slab deflection is 22.22 mm, but in the experimental model, it is 24.23 mm. The slab was investigated experimentally and analytically under two-point loading, the results are presented below. Table 2 shows the loads and deflections for plain and CHRRC slab specimens. Figure 9 depicts deforming CHRRC slabs.

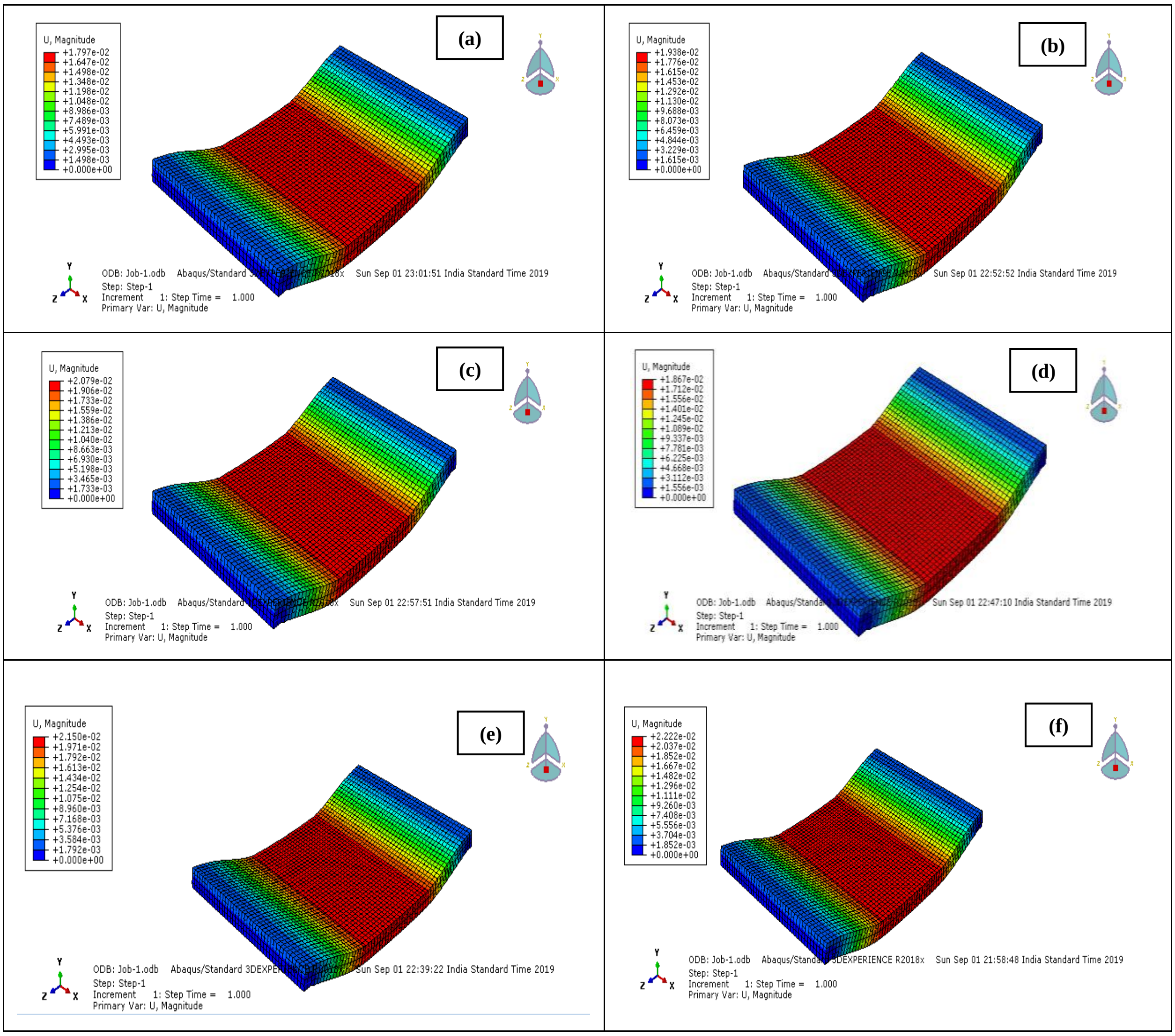

Fig. 9: Deflection plots of CHRRCS slabs (a) ORCS1, (b) CHRRCS1, (c) CHRRCS2, (d) CHRRCS3, (e) CHRRCS4 and (f) CHRRCS5

Table 2. Comparison of experimental and ABAQUS results under flexural load

S. No.	Slab ID	Type of Slab	Grade of concrete	Slab Dimension (mm)	Ultimate Load (kN)	Deflection (mm)		
						EXP (a_{exp})	FEA (a_{FEM})	(a_{FEM})/(a_{exp})
1	ORCS1	OWS	M30	1000 × 450 × 60	19.4	9.13	8.45	0.91
2	CHRRCS1				20.1	9.26	8.74	0.93
3	CHRRCS2				22.2	10.51	9.94	0.93
4	CHRRCS3				21.2	10.12	9.49	0.94
5	CHRRCS4				23.2	11.03	10.38	0.95
6	CHRRCS5				25.1	11.43	10.85	0.96

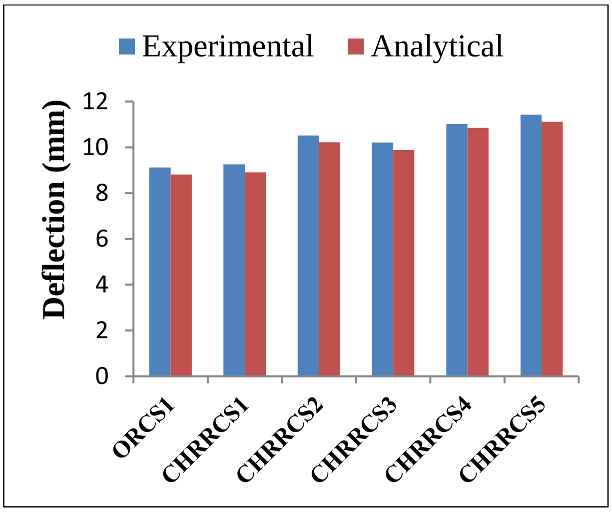

Fig. 10: Deflections in ORCS and C-HRRCS

Figure 10 depicts the deflection values of ORC and CHRRC slabs. The CHRRCS with 10 % ceramic replacement and 2.0 % rubber fibers have a higher flexural strength than conventional concrete slabs. Regular reinforced concrete slabs have a lower flexural strength than CHRRCS5. For static loads versus displacement behaviour, the experimental findings were quite close to the ABAQUS predictions (Al-Tayeb *et al.* 2013). The ABAQUS modelling and testing results were determined to be satisfactory. The current ABAQUS (FEA) model can simulate CHRRC slab behaviour.

4. CONCLUSION

The test results of the conventional slab and the CHRRC slabs have been tested and compared with the FEA. The load-carrying capacity of CHRRC slabs is improved by increasing the ceramic and rubber fiber content in both analytical and experimental experiments. The CHRRC slabs with 10% ceramic powder, 10% treated crumb rubber and 2% rubber fiber likely to have higher ultimate loads and deflection under flexural stress, when compared with the conventional concrete slabs and all other slabs. The FEA analysis is almost the same when compared to the experimental results.

FUNDING

This research received no specific grant from any funding agency in the public, commercial, or not-for-profit sectors.

CONFLICTS OF INTEREST

The authors declare that there is no conflict of interest.

REFERENCES

Ali, O. A. and Ayhan, O. Y., Crumb rubber in concrete: Static and dynamic evaluation, *Constr. Build. Mater.*, 36, 617-622 (2012). https://doi.org/10.1016/j.conbuildmat.2012.04.068

Al-Tayeb, M. M., Abu, B. B. H., Akil, H. M. and Ismail, H., Performance of Rubberized and Hybrid Rubberized Concrete Structures under Static and Impact Load Conditions, *Exp. Mech.*, 53, 377-384 (2012). https://doi.org/10.1007/s11340-012-9651-z

Al-Tayeb, M. M., Abu, B. B. H., Ismail, H. and Akil, H. M., Effect of Partial Replacement of Sand by Recycled Fine Crumb Rubber on the Performance of Hybrid Rubberized-Normal Concrete under Impact Load: Experiment and Simulation, *J. Cleaner Prod.*, 59, 284-289 (2013). http://dx.doi.org/10.1016%2Fj.jclepro.2013.04.026

Awoyera, P. O., Akinmusuru, J. O. and Ndambuki, J. M., Green concrete production with ceramic wastes and laterite, *Constr. Build. Mater.*, 117, 29-36 (2016). https://doi.org/10.1016/j.conbuildmat.2016.04.108

Aziz, I. A. and Salwa, H. A., Effect of Rubber Treated by Acidic Solution on Some Mechanical Properties of Rubberize Cement Mortar, *Eng. Tech. J.*, 29(13), 2793-2806 (2011).

Aziz, I. A., Wisam, A. A. and Salwa, Hadi, A., Cement Mortar Properties Contain Crumb Rubber Treated with Alkaline, Mater, *Mod. Appl. Sci.*, 4(12), 156-163 (2010). https://doi.org/10.5539/mas.v4n12p156

Camille, A. I. and George, S., Utilization of Recycled Crumb Rubber as Fine Aggregates in Concrete Mix Design, *Constr. Build. Mater.*, 42, 48-52 (2013). https://doi.org/10.1016/j.conbuildmat.2012.12.054

Eldin, N. N. and Senouci, A. B., Rubber-tyre Particles as Concrete Aggregate, J. *Mater. Civ. Eng.*, 5(2), 478-496 (1993).

El-Gammal, A, Abdel-Gawas, A. K., El-Sherbini, Y. and Shalaby, A., Compressive Strength of Concrete Utilizing Waste Tyre Rubber, Journal of Emerg, *Trends Engineering Applied Science*, 1(1), 96–99 (2010).

EPA, Markets for Scrap Tyres, US Environmental Protection Agency, Office of Solid Waste, Washington DC (1991).

Ganesan, N, Bharati, R. J. and Shashikala, Strength and Durability of Self-Compacting Rubberized Concrete, *The Indian Concrete Journal*, 86(9), 15-24 (2012).

IS 10262:2009, Recommended Guidelines for Concrete Mix Design, Bureau of Indian Standards, New Delhi.

IS 456:2000, Plain and Reinforced Concrete–Code of Practices, Bureau of Indian Standards, New Delhi.

IS 516:1959, Method of Tests for Strength of Concrete, Bureau of Indian Standards, New Delhi.

Kamil, E. K., George, B. W. and Han, Z., Properties of Crumb Rubber Concrete, *Transp. Res. Rec.*, 1914(1), 8-14 (2005). https://doi.org/10.1177/0361198105191400102

Kim, W., Villalobos, G., Baker, C., Frantz, J., Shaw, B., Bayya, S. and Sanghera, J., Overview of transparent optical ceramics for high-energy lasers at NRL, *Appl. Opt.*, 54(31), 210-221 (2015). http://dx.doi.org/10.1364/AO.54.010618

Rashid, K., Razzaq, A., Ahmad, M., Rashid, T. and Tariq, S., Experimental and analytical selection of sustainable recycled concrete with ceramic waste aggregate, *Constr. Build. Mater.*, 154, 829-840 (2017). https://doi.org/10.1016/j.conbuildmat.2017.07.219

Sara, S. G., Giuseppe, C. M., Massimo, B. and Marcello, M., Use of Rubber Particles from Recycled Tires as a Concrete Aggregate for Engineering Applications, Second international Conference on Sustainable construction materials and Technologies, The University of Wisconsin Milwaukee Centre of Byproducts Utilization (2010).

Sergio, A. Z. C. and Rolando, S. E., Luis, C. S. H., Roberto, A. M. A., Erick, M. H., Enriqueta, Y. C. and Agustín, L. H. M., Sustainable development of concrete through aggregates and innovative materials: A review, *Appl. Sci.*, 11(2), 1-28 (2021). https://doi.org/10.3390/app11020629

Vejmelková, E., Keppert, M., Rovnaníková, P., Ondráček, M., Keršner, Z. and Černý, R., Properties of high-performance concrete containing fine-ground ceramics as supplementary cementitious material, *Cem. Concr. Compos.*, 34(1), 55-61 (2012). http://dx.doi.org/10.1016%2Fj.cemconcomp.2011.09.018